Astronomy & Astrophysics manuscript no. ms˙rv2˙nigel
August 5, 2011

R-matrix electron-impact excitation data for astrophysically abundant sulphur ions⋆

G.Y. Liang[1], N.R. Badnell[1], G. Zhao[2], J.Y. Zhong[2] and F.L. Wang[2]

[1] Department of Physics, University of Strathclyde, Glasgow, G4 0NG, UK
[2] National Astronomical Observatories, CAS, Beijing, 100012, China
e-mail: gyliang@bao.ac.cn, gzhao@bao.ac.cn

Received date / Accepted date:

ABSTRACT

Aims. We present results for the electron-impact excitation of highly-charged sulphur ions (S^{8+}–S^{11+}) obtained using the intermediate-coupling frame transformation *R*-matrix approach.
Methods. A detailed comparison of the target structure has been made for the four ions to assess the uncertainty on collision strengths from the target structure. Effective collision strengths (Υs) are presented at temperatures ranging from $2\times10^2(z+1)^2$ K to $2\times10^6(z+1)^2$ K (where z is the residual charge of ions).
Results. Detailed comparisons for the Υs are made with the results of previous calculations for these ions, which will pose insight on the uncertainty in their usage by astrophysical and fusion modelling codes.
Conclusions.

Key words. atomic data – atomic processes – plasmas

1. Introduction

Many extreme ultraviolet (EUV) lines due to $n = 2 \rightarrow 2$ transitions of highly-charged sulphur ions have been recorded in solar observations (Thomas & Neupert 1994, Brown et al. 2008). Some transition lines show diagnostic potential for electron density, e.g. the emission lines of S XII (Keenan et al. 2002). Additionally, a few soft X-ray emission lines due to $n = 3 \rightarrow 2$ transitions of sulphur ions have also been detected in solar observations (Acton et al. 1985) and a *Chandra* Procyon observation (Raassen et al. 2002). However, most of the excitation data adopted in astrophysical modelling for sulphur spectra are from the distorted-wave (DW) method, which is well known to underestimate results for weaker transitions compared to those from an *R*-matrix calculation. Only data from a few small *R*-matrix calculations is available for sulphur ions to-date.

For S^{8+}, Bhatia & Landi (2003a) reported an extensive excitation calculation (n=3) with the DW method, which is currently used by astrophysical modelling codes, e.g. CHIANTI v6 (Dere et al. 2009). *R*-matrix data is available only for transitions within the ground configuration (Butler & Zeippen 1994).

For S^{9+}, DW excitation data for transitions of levels up to $n = 3$ were calculated by Bhatia & Landi (2003b), which were also incorporated into CHIANTI v6. An *R*-matrix calculation has been performed by Bell & Ramsbottom (2000), but only data for transitions among levels of n=2 complex and $2s^22p^23s$ configuration were reported.

For S^{10+}, the newest excitation data are attributed to be the work of Landi & Bhatia (2003), who have extended a previous (n=3) DW calculation to include n=4 configurations (viz $2s^22p4l'$, l'=s, p and d). Their results have been incorporated into astrophysical modelling codes, e.g. CHIANTI v6. By using *R*-matrix results available for some carbon-like ions (e.g. O^{2+}, Ne^{4+}, Mg^{6+}, Si^{8+} and Ca^{14+}), Conlon et al. (1992) derived the electron excitation data for other carbon-like ions, including S^{10+}, by interpolation. These resultant data are only valid for a range of electron temperatures approximately equal to $\log T_{\max} \pm 0.8$dex, where $T_{\max}$ is the temperature of maximum fractional abundance in ionization equilibrium. However, interpolation and/or extrapolation from *R*-matrix calculations was proved to be invalid at low temperatures because of the complexity of effective collision strengths along the iso-electronic sequence, as shown in Li-like (Liang & Badnell 2011), F-like (Witthoeft et al. 2007), Ne-like (Liang & Badnell 2010) and Na-like (Liang et al. 2009b) iso-electronic sequences. An explicit *R*-matrix calculation for this ion for transitions between levels of the n=2 complex was reported by Lennon & Burke (1994).

For S^{11+}, the *R*-matrix calculations by Zhang et al. (1994) and Keenan et al. (2002) are still the main data source for modelling — the close-coupling expansion included the lowest 8 LS terms of the n=2 complex. However, there are potential problems for B-like ions as demonstrated by Liang et al. (2009a) for Si^{9+}, viz. effective collision strengths of a previous *R*-matrix calculation (Keenan et al. 2000) do not converge to the correct high-temperature limit for a few strong transitions.

Here, we report-on calculations for the electron-impact excitation of four iso-nuclear ions of sulphur (S^{8+}—S^{11+}) which were made using the ICFT *R*-matrix method. The remainder of this paper is organized as follows. In Sect. 2 and 3, we discuss details of the calculational method and pay particular attention to comparing our underlying atomic structure results with those of previous workers. The model for the scattering calculation is outlined in Sect. 4. The excitation results themselves are discussed in Sect. 5 and we summarise in Sect. 6.

⋆ These data are made available in the archives of APAP via http://www.apap-network.org, OPEN-ADAS via http://open.adas.ac.uk as well as anonymous ftp to cdsarc.u-strasbg.fr (130.79.128.5) or via http://cdsweb.u-strasbg.fr/cgi-bin/qcat?J/A+A/

Table 2. Radial scaling parameters for S^{8+} – S^{11+} ions.

Orbitals	S^{8+}	S^{9+}	S^{10+}	S^{11+}
1s	1.46525	1.432	1.39497	1.38787
2s	1.25277	1.339	1.22509	1.24802
2p	1.16771	1.266	1.15638	1.17263
3s	1.21916	1.232	1.43868	1.60433
3p	1.14234	1.186	1.26648	1.36255
3d	1.16786	1.281	1.33814	1.47452
4s	1.24628	1.232	1.36150	1.47343
4p	1.15464	1.189	1.23441	1.36462
4d	1.12290	1.274	1.30375	1.53091
4f	1.13233	1.289	1.09803	1.39692

2. Structure: Level energy

The target radial wavefunctions (1s – 4f) were obtained from AUTOSTRUCTURE (hereafter AS, Badnell 1986) using the Thomas-Femi-Dirac-Amaldi model potential. Relativistic effects were included perturbatively from the one-body Breit–Pauli operator (viz. mass-velocity, spin-orbit and Darwin) without valence-electron two-body fine-structure operators. This is consistent with the operators included in the standard Breit–Pauli *R*-matrix suite of codes.

2.1. S IX

Configuration interaction among 30 configurations (see Table 1) was included to describe the target used to calculate level energies and weighted absorption oscillator strengths ($g_i f_{ij}$, for a given $i \leftarrow j$ transition). The model potential radial scaling parameters, λ_{nl} ($n = 1-4$; $l \in$ s, p, d, and f), were obtained by a three-step optimization procedure. In the first step, the energy of the $2s^x2p^y$ ($x + y = 6$) was minimized by varying the λ_{1s}, λ_{2s} and λ_{2p} scaling parameters. Then, the energies of the $2s^22p^33l$ and $2s^22p^34l$ configurations were minimized by varying the λ_{3l} and λ_{4l} scaling parameters, respectively. The resultant scaling parameters are listed in Table 2.

The 92 lowest-lying fine-structure target levels of $2s^x2p^y$ ($x+y = 6$), $2s^22p^33l$ and $2s2p^43s$ (^{5}P and ^{3}P, only) configurations were used in the close-coupling expansion for the scattering calculation. The resultant level energies are compared with experimentally derived data from NIST v4[1] and previous calculations, see Table 3. The present AS level energies show an excellent agreement (less than 0.5% except for $2s^22p^4\ ^3$P) with those of Bhatia & Landi (2003a). This is due to the use of similar structure codes and calculations. The main difference between the two is the $n = 4$ configurations that we included in our CI expansion but were not used by Bhatia & Landi (2003a).

When compared with NIST data and the MCHF collection [2] (Tachiev & Froese Fischer, 2002), the present results agree to within 1% for all levels of the n=3 configurations. For levels of the n=2 configurations, the energy difference is about 2–5%. So, we performed a calculation with energy corrections to the diagonal of the Hamiltonian matrix before diagonalization, for the 16 lowest-lying levels, and iterated to convergence. For the missing level ($2s^22p^33s\ ^5S_2$) in the NIST compilation, we adopt the mean value of differences between our level energies and corresponding NIST values of the same configuration. The resultant e-vectors and e-energies are used to calculate the oscillator strengths and archived energies.

[1] http://physics.nist.gov/PhysRefData/ASD/levels_form.html
[2] http://nlte.nist.gov/MCHF/

We notice that the MCHF data shows an excellent agreement with the data compiled in the NIST database. A non-relativistic multi-configuration Hartree–Fock (MCHF) approach was used by Tachiev & Froese Fischer (2002) to generate radial orbitals for subsequent use in diagonalizing a smaller scale Breit–Pauli Hamiltonian. A large set of configurations was used in the LS-coupling calculation, for example, configuration states were included up to $n = 7$. Orbitals sets were optimized separately for the initial and final states and no orthonormality was imposed between the two sets. Thus, we consider this MCHF data to be the theoretical reference work.

2.2. S X

Configuration interaction among 24 configurations (see Table 1) was included to calculate the level energies and oscillator strengths between levels of the configurations $2s^x2p^y$ ($x+y = 5$) and $2s^22p^23l$. Since the same configuration interaction and a similar structure code (SUPERSTRUCTURE) was used by Bhatia & Landi (2003b), we use their scaling parameters λ_{nl} in the present work for this ion. We note that there is severe interaction between the $2s^22p^23l$ and $2s2p^33l'$ configurations. So some terms of the $2s2p^33s$ (^{6}S, ^{4}S and ^{4}D) and $2s2p^33p$ (^{6}P and ^{4}D) configurations were included in the close-coupling expansion for the excitation calculation, as detailed in the next section.

The calculated energies for the 84 lowest-lying levels are listed in Table 4 along with experimentally derived data from the NIST v4 compilation as well as other predictions. Although we have used the same configuration expansion and same radial orbitals as Bhatia & Landi (2003b), the energies do not quite match because we have omitted all two-body fine-structure operators so as to be consistent with our subsequent *R*-matrix calculation. (If we include them for the 3 configurations of the ground complex then we reproduce their energies.) The difference is much smaller than the difference with the experimentally derived NIST energies. When compared with the NIST compilation [1] and the MCHF collection [2], both agree to within 0.5% for all levels of the $n = 3$ configurations. For the levels of $n = 2$ complex, the difference is up to about 5%. So, we again iterated with energy corrections to the diagonal of Hamiltonian matrix before diagonalization, for the 22 lowest-lying levels, to calculate oscillator strengths and archived energies. The data of MCHF collection (Tachiev & Froese Fischer 2002) shows an excellent agreement again with the NIST data.

2.3. S XI

As shown in Table 1, configuration interaction among 24 configurations has been taken into account to calculate the level energies and oscillator strengths. The radial scaling parameters λ_{nl} were obtained by a three-step optimization procedure. In the first step, the energy of the $2s^x2p^y$ ($x+y = 4$) was minimized by varying the λ_{1s}, λ_{2s} and λ_{2p} scaling parameters. Then, the energies of the $2s^22p3l$ and $2s^22p4l$ configurations were minimized by varying the λ_{3l} and λ_{4l} scaling parameters, respectively. The resultant scaling parameters are listed in Table 2.

The 254 lowest-lying fine-structure levels were used in the close-coupling expansion for the scattering calculation. They are compared with those data available from the NIST compilation and other predictions in Table 5. The present calculation shows a good agreement (1%) with those experimentally determined data in NIST database and the MCHF collection[2] for $2s2p^3\ ^3$D, ^{3}P and $n = 3, 4$ levels. For other levels of the $2s2p^3$ configura-

Table 1. Configurations included in the CC and CI expansions for S^{8+} – S^{11+} ions.

	CC configurations	additional CI configuration
S IX	$2s^x2p^y$ ($x+y=6$)	$2s^22p^34l$, $2s2p^43s$ (except for ^{5}P and ^{3}P)
	$2s^22p^33l$	$2s2p^4\{3p, 3d, 4l\}$
	$2s2p^43s$ (^{5}P and ^{3}P)	$2p^5\{3,4\}l$
		$2s^22p^23l^x3l'^y$ ($x+y=2$)
S X	$2s^x2p^y$ ($x+y=5$)	$2s2p^3\{3,4\}l$
	$2s^22p^23l$	$2s^22p^24l$
	$2s2p^33s$ (^{6}S, ^{4}S and ^{4}D)	$2p^4\{3,4\}l$
	$2s2p^33p$ (^{6}P and ^{4}P)	
S XI	$2s^x2p^y$ ($x+y=4$)	$2p^33p$ (^{1}D, ^{1}S)
	$2s^22p3l$, $2s2p^23l$	$2p^33p$ (^{3}S, ^{1,3}P/D/F)
	$2s^22p4l$, $2p^33s$	$2s2p^24l$
	$2p^33p$ (except for ^{1}D, ^{1}S)	$2p^34l$
	$2p^33d$ (except for ^{3}S, ^{1,3}P/D/F)	
S XII	$2s^x2p^y$ ($x+y=3$)	$2p^23\{4\}l$, $2s3s3l$
	$2s^23\{4\}l$, $2s2p3\{4\}l$	$2p3s3l$, $2s3p^2$, $2s3d^2$

tion and those of the $2p^4$ configuration, the present results are systematically higher than NIST data by 1–2%. The present AS result shows an excellent agreement (less than 0.5%) with the result of Landi & Bhatia (2003) for all levels of the n=3 configurations. However, both sets of results are systematically higher than the NIST data for the levels of n=2 complex, those of Landi & Bhatia (2003) more-so than the present which are within 2% (excluding the $^5S_2$). So, we perform an iterated energy correction calculation again for the 23 lowest-lying excited levels.

The data of MCHF collection show better agreement again with the NIST data than other predictions. Unfortunately, there are no published papers to indicate the scale of calculations.

2.4. S XII

Configuration interaction among 32 configurations has been taken into account to calculate level energies and oscillator strengths, see Table 1. The radial scaling parameters λ_{nl} were obtained by a three-step optimization procedure. In the first step, the energy of the $2s^x2p^y$ ($x+y=3$) configurations was minimized by varying the λ_{1s}, λ_{2s} and λ_{2p} scaling parameters. Then, the energies of the $2s^22p3l$ and $2s^22p4l$ configurations were minimized by varying the λ_{3l} and λ_{4l} scaling parameters, respectively. The resultant scaling parameters are listed in Table 2.

The 204 lowest-lying target levels were used in the close-coupling expansion for the scattering calculation. The present AS level energies are compared with those data available from the NIST compilation and other predictions, see Table 6. A good agreement (less than 1%) is obtained when compared with those experimentally determined in the NIST database for levels of the n=3 configurations. For levels of the $n=2$ complex, the difference is slightly larger, but still within ∼2%. Comparison with data in CHIANTI v6[3] demonstrates that the differences are within 1% for almost all levels except for those of the n=2 complex. A good agreement is found when compared with calculations by Merkelis et al. (1995) with many-body perturbation theory (MBPT) and all-order relativistic many-body theory by Nataraj et al. (2007). As done for other ions, energy corrections for the levels of $2s^x2p^y$ ($x+y$=3) configurations have been included to improve the accuracy of the oscillator strengths and archived energies.

[3] Database comments denote that the gf compilation for S^{11+} is from an unpublished calculation by Zhang et al. Additionally, the level energies of the n=2 complex are the observed ones and not the theoretical values, as stated in this database.

3. Structure: Oscillator strengths

A further test of our structure calculation is to compare weighted oscillator strengths gf_{ij}. In terms of the transition energy E_{ji} (Ryd) for the $j \rightarrow i$ transition, the transition probability or Einstein's A-coefficient, A_{ji} can be written as

$$A_{ji}(\text{au}) = \tfrac{1}{2}\alpha^3 \frac{g_i}{g_j} E_{ji}^2 f_{ij}, \quad (1)$$

where α is the fine structure constant, and g_i, g_j are the statistical weight factors of the initial and final states, respectively.

Figure 1 shows such a comparison for the transitions into the five lowest-lying levels for the four iso-nuclear ions to assess the accuracy of the structure calculation. For S^{8+}, about 86% of all available transitions in the work of Bhatia & Landi (2003a) show agreement to within 20%. When compared with the data from the MCHF collection[2], 61% of all available transitions agree to within 20%. For those transitions with larger differences in the two cases, the data points are linked together by a solid line. For some transitions, the present results agree better with the results of Bhatia & Landi (2003a) than with the data from MCHF collection, while for others they agree better with the data from the MCHF method. Since correlation from much higher excited configuration has been taken into account in the data of MCHF collection, their gf-values are the best transition data so-far, as demonstrated by their level energies. The present results show a better agreement with MCHF calculation (Tachiev & Froese Fischer, 2002) than those of Bhatia & Landi (2003a), which indicates that we have a more accurate structure.

Table 3. Level energies (Ryd) of S^{8+} from different calculations along with experimentally derived values from NIST v4.

ID	Specification	NIST[1]	AS	MCHF[a]	BL03[b]	ID	Specification	NIST	AS	MCHF	BL03
1	$2s^22p^4\ ^3P_2$		0			47	$2s^22p^3(^4S)3d\ ^5D_4$		18.2653	18.3135	18.2392
2	$2s^22p^4\ ^3P_1$	0.07276	0.0730	0.0731	0.0755	48	$2s^22p^3(^2D)3p\ ^1P_1$		18.2871	18.3379	18.2616
3	$2s^22p^4\ ^3P_0$	0.097032	0.0981	0.0968	0.1005	49	$2s^22p^3(^2D)3p\ ^3P_2$		18.3578	18.4164	18.3383
4	$2s^22p^4\ ^1D_2$	0.531213	0.5601	0.5353	0.5625	50	$2s^22p^3(^2D)3p\ ^3P_1$		18.3728	18.4217	18.3583
5	$2s^22p^4\ ^1S_0$	1.1181	1.1229	1.1177	1.1318	51	$2s^22p^3(^2D)3p\ ^3P_0$		18.3808	18.4251	18.3685
6	$2s2p^5\ ^3P_2$	4.05502	4.1504	4.0671	4.1505	52	$2s^22p^3(^4S)3d\ ^3D_2$	18.5464	18.5248	18.5519	18.5046
7	$2s2p^5\ ^3P_1$	4.11888	4.2172	4.1312	4.2165	53	$2s^22p^3(^4S)3d\ ^3D_1$	18.5475	18.5265	18.5542	18.5065
8	$2s2p^5\ ^3P_0$	4.15438	4.2528	4.1669	4.2530	54	$2s^22p^3(^4S)3d\ ^3D_3$	18.5522	18.5321	18.5585	18.5119
9	$2s2p^5\ ^1P_1$	5.61407	5.8016	5.6353	5.7982	55	$2s^22p^3(^2D)3p\ ^1D_2$		18.6042	18.5960	18.5981
10	$2p^6\ ^1S_0$	9.470060	9.7908	9.5003	9.7967	56	$2s^22p^3(^2D)3p\ ^1S_0$		18.9893	18.9748	18.9813
11	$2s^22p^3(^4S)3s\ ^5S_2$		15.9343	16.0032	15.9188	57	$2s^22p^3(^4S)3d\ ^3F_2$		19.0114	19.0399	18.9807
12	$2s^22p^3(^4S)3s\ ^3S_1$	16.2493	16.2047	16.2520	16.1900	58	$2s^22p^3(^4S)3d\ ^3F_3$		19.0287	19.0537	18.9982
13	$2s^22p^3(^4S)3s\ ^3D_1$	16.8126	16.7815	16.8207	16.7656	59	$2s^22p^3(^2D)3d\ ^1S_0$		19.0460	19.0621	19.0154
14	$2s^22p^3(^4S)3s\ ^3D_2$	16.8144	16.7845	16.8225	16.7625	60	$2s^22p^3(^2D)3d\ ^3F_4$		19.0493	19.0701	19.0191
15	$2s^22p^3(^4S)3s\ ^3D_3$	16.8208	16.7950	16.8289	16.7761	61	$2s^22p^3(^2D)3d\ ^3G_3$		19.1082	19.1308	19.0799
16	$2s^22p^3(^2D)3s\ ^1D_2$	16.9386	16.9211	16.9480	16.9024	62	$2s^22p^3(^2D)3d\ ^3G_4$		19.1145	19.1344	19.0864
17	$2s^22p^3(^4S)3p\ ^5P_1$		16.9639	17.0182	16.9377	63	$2s^22p^3(^2D)3d\ ^3G_5$		19.1218	19.1377	19.0939
18	$2s^22p^3(^4S)3p\ ^5P_2$		16.9696	17.0242	16.9438	64	$2s^22p^3(^2D)3d\ ^1G_4$		19.1466	19.1597	19.1210
19	$2s^22p^3(^4S)3p\ ^5P_3$		16.9795	17.0352	16.9542	65	$2s^22p^3(^2D)3d\ ^3D_1$	19.1852	19.1769	19.2311	19.1507
20	$2s^22p^3(^4S)3s\ ^3P_0$		17.1515	17.2265	17.1317	66	$2s^22p^3(^2D)3d\ ^3D_2$	19.2106	19.2066	19.2224	19.1816
21	$2s^22p^3(^4S)3s\ ^3P_1$		17.1577	17.2315	17.1378	67	$2s^22p^3(^2D)3d\ ^3D_3$	19.2117	19.2152	19.2257	19.1912
22	$2s^22p^3(^4S)3s\ ^3P_2$	17.2396	17.1736	17.2447	17.1536	68	$2s^22p^3(^2D)3d\ ^1P_1$	19.2177	19.2191	19.1974	19.1937
23	$2s^22p^3(^4S)3p\ ^3P_1$		17.2128	17.2521	17.1940	69	$2s^22p^3(^2D)3d\ ^1D_2$	19.2954	19.2740	19.3080	19.2480
24	$2s^22p^3(^4S)3p\ ^3P_2$		17.2171	17.2555	17.1983	70	$2s^22p^3(^2D)3d\ ^3P_2$	19.2865	19.2876	19.3004	19.2630
25	$2s^22p^3(^4S)3p\ ^3P_0$		17.2184	17.2585	17.1999	71	$2s^22p^3(^2D)3d\ ^3P_1$	19.3128	19.3153	19.3249	19.2908
26	$2s^22p^3(^2D)3s\ ^1P_1$	17.3533	17.2987	17.3625	17.2788	72	$2s^22p^3(^2D)3d\ ^3P_0$		19.3178	19.3283	19.2929
27	$2s^22p^3(^4S)3p\ ^1P_1$		17.6866	17.7191	17.6583	73	$2s^22p^3(^2D)3d\ ^3S_1$	19.3693	19.3521	19.3829	19.3291
28	$2s^22p^3(^2D)3p\ ^3D_2$		17.7395	17.7706	17.7221	74	$2s^22p^3(^2D)3d\ ^1F_3$	19.4529	19.4622	19.4678	19.4390
29	$2s^22p^3(^2D)3p\ ^3D_1$		17.7499	17.7808	17.7109	75	$2s2p^4(^4P)3s\ ^5P_3$		19.4781		
30	$2s^22p^3(^2D)3p\ ^3D_3$		17.7588	17.7866	17.7305	76	$2s^22p^3(^2D)3d\ ^3F_4$		19.4928	19.5456	19.4632
31	$2s^22p^3(^4S)3p\ ^3F_2$		17.8168	17.8469	17.7910	77	$2s^22p^3(^2D)3d\ ^3P_0$	19.5264	19.4967	19.5583	19.4673
32	$2s^22p^3(^4S)3p\ ^3F_3$		17.8289	17.8575	17.8032	78	$2s^22p^3(^2D)3d\ ^3F_2$		19.5004	19.5554	19.4708
33	$2s^22p^3(^4S)3p\ ^3F_4$		17.8422	17.8683	17.8169	79	$2s^22p^3(^2D)3d\ ^3F_3$		19.5060	19.5542	19.4798
34	$2s^22p^3(^2D)3p\ ^1F_3$		17.8742	17.9008	17.8518	80	$2s^22p^3(^2D)3d\ ^3P_1$	19.5449	19.5118	19.5705	19.4828
35	$2s^22p^3(^4S)3p\ ^3S_1$		18.0829	18.2133	18.0569	81	$2s^22p^3(^2D)3d\ ^3P_2$	19.5613	19.5296	19.5851	19.5004
36	$2s^22p^3(^2D)3p\ ^3P_0$		18.1322	18.1492	18.1138	82	$2s2p^4(^4P)3s\ ^5P_2$		19.5299		
37	$2s^22p^3(^2D)3p\ ^3P_2$		18.1596	18.1624	18.1468	83	$2s2p^4(^4P)3s\ ^5P_1$		19.5629		
38	$2s^22p^3(^2D)3p\ ^3P_1$		18.1770	18.1262	18.1570	84	$2s^22p^3(^2D)3d\ ^3D_2$	19.6340	19.6039	19.6485	19.5786
39	$2s^22p^3(^2D)3p\ ^3D_1$		18.1936	18.2533	18.1659	85	$2s^22p^3(^2D)3d\ ^3D_3$	19.6508	19.6167	19.6642	19.5907
40	$2s^22p^3(^2D)3p\ ^3D_2$		18.1958	18.2505	18.2390	86	$2s^22p^3(^2D)3d\ ^3D_1$	19.6493	19.6183	19.6651	19.5936
41	$2s^22p^3(^2D)3p\ ^3D_3$		18.2102	18.2710	18.1828	87	$2s^22p^3(^2D)3d\ ^1D_2$	19.7085	19.6963	19.7220	19.6733
42	$2s^22p^3(^2D)3p\ ^1D_2$		18.2561	18.2975	18.1694	88	$2s^22p^3(^2D)3d\ ^1F_3$	19.7429	19.7241	19.7557	19.7042
43	$2s^22p^3(^4S)3d\ ^5D_0$		18.2617	18.3130	18.2352	89	$2s2p^4(^4P)3s\ ^3P_2$		19.8880		
44	$2s^22p^3(^4S)3d\ ^5D_1$		18.2620	18.3131	18.2356	90	$2s2p^4(^4P)3s\ ^3P_1$		19.9453		
45	$2s^22p^3(^4S)3d\ ^5D_2$		18.2627	18.3131	18.2364	91	$2s^22p^3(^2D)3d\ ^1P_1$	19.9588	19.9473	19.9727	19.9269
46	$2s^22p^3(^4S)3d\ ^5D_3$		18.2638	18.3131	18.2375	92	$2s2p^4(^4P)3s\ ^3P_0$		19.9718		

[a] Refers to data from the MCHF collection [2].

[b] Refers to the work of Bhatia & Landi (2003a).

For S^{9+}, 82% of transitions agree to within 20% for the present AS results and those of Bhatia & Landi (2003b). Recall, we omitted two-body fine-structure but have iterated to the observed energies, for levels of the ground complex, compared to Bhatia & Landi (2003b). We have also performed calculations with/without the two-body fine-structure and level energy corrections to study the effect of the two, see Table 7. It appears that the energy corrections play an more important on the resultant gf-value for these weak transitions. When compared with the data from the MCHF collection[2], about 64% of all available transitions show agreement to within 20%. For those transitions with larger differences, the data points are linked together as done for S^{8+}. We also notice that the level label for $2s^22p^23s\ ^2D_{5/2}$ (21^{th} in the Table 4) and $^2D_{3/2}$ (22^{th}) in MCHF collection should be exchanged because a good agreement between the MCHF calculation and the other two predictions can be obtained after such a procedure for all transitions to the five lowest-lying levels from the two levels, e.g. the 22→3 and 21→3 transitions marked in Fig. 1.

For S^{10+}, most (67%) transitions are in agreement to within 20% for the present AS results and those of Landi & Bhatia (2003). When compared with calculation from MCHF method, the percentage is about 90% of available transition data.

Table 4. Level energies (Ryd) of S^{9+} from different calculations along with experimentally derived values from NIST v4.

ID	Specification	NIST[1]	AS	BL03[a]	MCHF[b]	ID	Specification	NIST	AS	BL03	MCHF
1	$2s^22p^3\ ^4S_{3/2}$		0			43	$2s^22p^23p\ ^2P_{3/2}$		21.0732	21.0731	21.0498
2	$2s^22p^3\ ^2D_{3/2}$	0.751270	0.7929	0.7963	0.7568	44	$2s^22p^23d\ ^4F_{3/2}$		21.1123	21.1123	21.1308
3	$2s^22p^3\ ^2D_{5/2}$	0.761773	0.8101	0.8079	0.7681	45	$2s^22p^23d\ ^4F_{5/2}$		21.1338	21.1337	21.1511
4	$2s^22p^3\ ^2P_{1/2}$	1.15708	1.1932	1.1944	1.1597	46	$2s^22p^23d\ ^4F_{7/2}$		21.1661	21.1660	21.1818
5	$2s^22p^3\ ^2P_{3/2}$	1.17375	1.2131	1.2119	1.1765	47	$2s^22p^23d\ ^4F_{9/2}$		21.2102	21.2101	21.2225
6	$2s2p^4\ ^4P_{5/2}$	3.44876	3.4966	3.4954	3.4608	48	$2s2p^33s\ ^4S_{3/2}$		21.2346		21.2768
7	$2s2p^4\ ^4P_{3/2}$	3.51168	3.5593	3.5608	3.5239	49	$2s^22p^23d\ ^2P_{3/2}$	21.2431	21.2356	21.2355	21.2470
8	$2s2p^4\ ^4P_{1/2}$	3.54376	3.5933	3.5942	3.5557	50	$2s^22p^23d\ ^4D_{1/2}$		21.2421	21.2420	21.2611
9	$2s2p^4\ ^2D_{3/2}$	4.74518	4.8730	4.8739	4.7647	51	$2s^22p^23d\ ^4D_{5/2}$		21.2650	21.2649	21.2804
10	$2s2p^4\ ^2D_{5/2}$	4.74646	4.8771	4.8763	4.7660	52	$2s^22p^23d\ ^4D_{3/2}$		21.2826	21.2825	21.2943
11	$2s2p^4\ ^2S_{1/2}$	5.54765	5.6861	5.6864	5.5645	53	$2s^22p^23d\ ^4D_{7/2}$		21.2877	21.2877	21.3020
12	$2s2p^4\ ^2P_{3/2}$	5.80384	5.9722	5.9715	5.8300	54	$2s^22p^23p\ ^2P_{3/2}$		21.3270	21.3269	
13	$2s2p^4\ ^2P_{1/2}$	5.88369	6.0544	6.0545	5.9101	55	$2s^22p^23p\ ^2P_{1/2}$		21.3303	21.3302	
14	$2p^5\ ^2P_{3/2}$	9.03293	9.2852	9.2860	9.0635	56	$2s^22p^23d\ ^2P_{1/2}$	21.3346	21.3351	21.3350	21.3404
15	$2p^5\ ^2P_{1/2}$	9.134286	9.3930	9.3914	9.1650	57	$2s^22p^23d\ ^2F_{5/2}$	21.3509	21.3598	21.3597	21.3576
16	$2s^22p^23s\ ^4P_{1/2}$	19.0223	18.9961	18.9959	19.0238	58	$2s^22p^23d\ ^4P_{5/2}$	21.4199	21.4117	21.4115	21.4157
17	$2s^22p^23s\ ^4P_{3/2}$	19.0674	19.0380	19.0379	19.0660	59	$2s^22p^23d\ ^4P_{3/2}$	21.4441	21.4359	21.4358	21.4399
18	$2s^22p^23s\ ^4P_{5/2}$	19.1224	19.0981	19.0979	19.1226	60	$2s^22p^23d\ ^2F_{7/2}$	21.4283	21.4375	21.4374	21.4341
19	$2s^22p^23s\ ^2P_{1/2}$	19.2560	19.2446	19.2445	19.2535	61	$2s^22p^23d\ ^4P_{1/2}$	21.4491	21.4484	21.4482	21.4518
20	$2s^22p^23s\ ^2P_{3/2}$	19.3234	19.3163	19.3161	19.3221	62	$2s2p^33p\ ^6P_{3/2}$		21.5973		21.7238
21	$2s^22p^23s\ ^2D_{5/2}$	19.6846	19.6882	19.6881	19.6950	63	$2s2p^33p\ ^6P_{5/2}$		21.6051		21.7299
22	$2s^22p^23s\ ^2D_{3/2}$	19.6768	19.6907	19.6905	19.6924	64	$2s2p^33p\ ^6P_{7/2}$		21.6169		21.7420
23	$2s^22p^23p\ ^2S_{1/2}$		19.8772	19.8771	19.8971	65	$2s^22p^23d\ ^2D_{3/2}$	21.6763	21.6959	21.6957	21.6829
24	$2s^22p^23p\ ^4D_{1/2}$		19.9500	19.9499	19.9770	66	$2s^22p^23d\ ^2D_{5/2}$	21.6872	21.7147	21.7145	21.6984
25	$2s^22p^23p\ ^4D_{3/2}$		19.9719	19.9718	19.9993	67	$2s^22p^23d\ ^2G_{7/2}$		21.8602	21.8601	21.8540
26	$2s^22p^23p\ ^4D_{5/2}$		20.0119	20.0118	20.0389	68	$2s^22p^23d\ ^2G_{9/2}$		21.8693	21.8692	21.8617
27	$2s^22p^23p\ ^4P_{1/2}$		20.0652	20.0651	20.0927	69	$2s^22p^23d\ ^2D_{3/2}$	21.9401	21.9623	21.9622	21.9494
28	$2s^22p^23p\ ^4D_{7/2}$		20.0659	20.0658	20.0902	70	$2s^22p^23d\ ^2D_{5/2}$	21.9533	21.9702	21.9701	21.9512
29	$2s^22p^23p\ ^4P_{3/2}$		20.0742	20.0741	20.1002	71	$2s2p^33p\ ^4P_{5/2}$	22.0342	21.9714		22.0584
30	$2s^22p^23p\ ^4P_{5/2}$		20.1104	20.1103	20.1344	72	$2s2p^33p\ ^4P_{3/2}$		21.9756		22.0633
31	$2s^22p^23p\ ^2D_{3/2}$		20.2002	20.2001	20.2102	73	$2s2p^33p\ ^4P_{1/2}$		21.9795		22.0670
32	$2s^22p^23s\ ^2S_{1/2}$		20.2363	20.2361	20.2976	74	$2s^22p^23d\ ^2F_{7/2}$	21.9531	21.9922	21.9921	21.9623
33	$2s^22p^23p\ ^4S_{3/2}$		20.2660	20.2658	20.2949	75	$2s^22p^23d\ ^2F_{5/2}$	21.9848	22.0203	22.0201	21.9959
34	$2s^22p^23p\ ^2D_{5/2}$		20.2749	20.2748	20.2843	76	$2s^22p^23d\ ^2P_{1/2}$		22.0850	22.0849	22.0813
35	$2s^22p^23p\ ^2P_{1/2}$		20.3736	20.3735	20.3840	77	$2s^22p^23d\ ^2P_{3/2}$		22.1096	22.1095	22.1060
36	$2s^22p^23p\ ^2P_{3/2}$		20.3755	20.3754	20.3831	78	$2s^22p^23d\ ^2S_{1/2}$		22.1807	22.1806	22.1599
37	$2s2p33s\ ^6S_{5/2}$		20.6098		20.7326	79	$2s2p^33s\ ^4D_{3/2}$		22.3358		
38	$2s^22p^23p\ ^2F_{5/2}$		20.6772	20.6771	20.6810	80	$2s2p^33s\ ^4D_{5/2}$		22.3365		
39	$2s^22p^23p\ ^2F_{7/2}$		20.6955	20.6954	20.7004	81	$2s2p^33s\ ^4D_{1/2}$		22.3368		
40	$2s^22p^23p\ ^2D_{3/2}$		20.8957	20.8956	20.8739	82	$2s2p^33s\ ^4D_{7/2}$		22.3429		
41	$2s^22p^23p\ ^2D_{5/2}$		20.8991	20.8990	20.8742	83	$2s^22p^23d\ ^2D_{5/2}$		22.4934	22.4933	22.5332
42	$2s^22p^23p\ ^2P_{1/2}$		21.0228	21.0227	21.0023	84	$2s^22p^23d\ ^2D_{3/2}$		22.5124	22.5123	22.5509

[a] Refers to the work of Bhatia & Landi (2003b).

[b] Refers to data from the MCHF collection [2].

For S^{11+}, the present AS results agree well (within 20%) with predictions from other sources including SUPERSTRUCTURE (the data in CHIANTI database, 94% of available transitions), MCHF[2] (87%), MBPT (Merkelis et al. 1995[4], 83%) and the relativistic coupled-cluster theory (Nataraj et al. 2007), for transitions between levels of the n=2 complex. For transitions from higher excited levels, e.g. n=3 configurations, only the unpublished calculation of Sampson & Zhang is available (from the CHIANTI database.) Fig. 1 illustrates that only 46% of available transitions show agreement to within 20%.

Additionally, we explicitly label some transitions with large differences in Fig. 1. They are all from the 50th and 52nd levels. We recall that we take configuration, total angular momentum and energy ordering to be the 'good' quantum numbers when level matching for comparisons. Exchanging the level matching for these two levels cannot eliminate the large difference now, unlike the case of S^{9+}. Level mixing (2s2p3s ^{2}P contributes 86% for the 50th, 2s2p3d ^{4}P contributes 90% for the 52nd) also can not explain this discrepancy for these strong transitions.

Thus, we believe the atomic structure of the four iso-nuclear ions to be reliable, and expect the uncertainty in collision strengths due to in accuracies in the target structure to be correspondingly small.

4. Scattering

The scattering calculations were performed using a suite of parallel intermediate-coupling frame transformation (ICFT) *R*-matrix codes (Griffin et al. 1998). We employed 40 continuum basis orbitals per angular momentum so as to represent

[4] http://open.adas.ac.uk

Table 5. Level energies (Ryd) of S^{10+} from different calculations along with experimentally derived values from NIST v4. *Note: only levels with available NIST data and other predictions are listed. The complete table can be available from CDS archives.*

ID	Specification	NIST[1]	AS	LB03[a]	MCHF[b]	ID	Specification	NIST	AS	LB03	MCHF
1	$2s^22p^2\ ^3P_0$		0			48	$2s2p^23s\ ^3P_0$		23.5543		
2	$2s^22p^2\ ^3P_1$	0.047459	0.0468	0.0493	0.0463	49	$2s2p^23s\ ^3P_1$		23.5855		
3	$2s^22p^2\ ^3P_2$	0.112889	0.1161	0.1171	0.1119	50	$2s2p^23s\ ^3P_2$	23.6090	23.6442		
4	$2s^22p^2\ ^1D_2$	0.611882	0.6406	0.6467	0.6133	51	$2s^22p3d\ ^1P_1$	23.5974	23.7660	23.6057	23.6054
5	$2s^22p^2\ ^1S_0$	1.21134	1.2242	1.2376	1.2114	52	$2s^22p3d\ ^1F_3$	23.5958	23.7845	23.6205	23.6002
6	$2s2p^3\ ^5S_2$	1.69724	1.6307	1.6534	1.6977	56	$2s2p^23p\ ^5D_2$	23.7613	23.8851		
7	$2s2p^3\ ^3D_2$	3.23569	3.2607	3.2886	3.2412	64	$2s2p^23p\ ^3D_3$	24.2379	24.3250		
8	$2s2p^3\ ^3D_1$	3.23832	3.2616	3.2911	3.2439	71	$2s2p^23s\ ^3D_3$	24.5154	24.5069		
9	$2s2p^3\ ^3D_3$	3.23819	3.2686	3.2920	3.2438	83	$2s2p^23d\ ^5P_3$	25.0339	25.1200		
10	$2s2p^3\ ^3P_0$	3.79950	3.8307	3.8625	3.8049	84	$2s2p^23d\ ^5P_2$	25.084	25.1391		
11	$2s2p^3\ ^3P_1$	3.79986	3.8335	3.8632	3.8052	86	$2s2p^23d\ ^5P_1$	25.084	25.1544		
12	$2s2p^3\ ^3P_2$	3.80380	3.8391	3.8676	3.8089	89	$2s2p^23d\ ^3F_2$	25.174	25.3020		
13	$2s2p^3\ ^1D_2$	4.83133	4.9362	4.9602	4.8413	91	$2s2p^23d\ ^3F_3$	25.207	25.3358		
14	$2s2p^3\ ^3S_1$	4.87728	4.9635	4.9810	4.8859	92	$2s2p^23d\ ^3F_4$	25.257	25.3825		
15	$2s2p^3\ ^1P_1$	5.39908	5.5099	5.5368	5.4087	95	$2s2p^23p\ ^1D_2$	25.420	25.4352		
16	$2p^4\ ^3P_2$	7.39677	7.4931	7.5395	7.4098	97	$2s2p^23p\ ^1F_3$	25.470	25.5594		
17	$2p^4\ ^3P_1$	7.47723	7.5708	7.6232	7.4897	106	$2s2p^23d\ ^3D_3$	25.514	25.6540		
18	$2p^4\ ^3P_0$	7.50561	7.6000	7.6530	7.5193	123	$2s2p^23d\ ^3F_4$	26.266	26.4556		
19	$2p^4\ ^1D_2$	7.91401	8.0543	8.1063	7.9285	129	$2s2p^23d\ ^1F_3$	26.353	26.5317		
20	$2p^4\ ^1S_0$	8.99180	9.1670	9.2198	9.0064	140	$2s2p^23d\ ^1D_2$	26.6167	26.8086		
21	$2s^22p3s\ ^3P_0$	21.2144	21.2187	21.0931	21.1163	158	$2s2p^23d\ ^3P_2$	27.8214	27.7608		
22	$2s^22p3s\ ^3P_1$	21.1438	21.2440	21.1182	21.1405	187	$2s^22p4s\ ^3P_0$		28.7144	28.5491	
23	$2s^22p3s\ ^3P_2$	21.2447	21.3275	21.2098	21.2337	189	$2s^22p4s\ ^3P_1$		28.7282	28.5618	
24	$2s^22p3s\ ^1P_1$	21.3698	21.4953	21.3574	21.3669	191	$2s^22p4s\ ^3P_2$		28.8229	28.6645	
25	$2s^22p3p\ ^1P_1$		22.0422	21.9292	21.9462	193	$2s^22p4s\ ^1P_1$		28.8753	28.7036	
26	$2s^22p3p\ ^3D_1$		22.1327	22.0180	22.0376	197	$2s^22p4p\ ^3D_1$		29.0558	28.8900	
27	$2s^22p3p\ ^3D_2$		22.1520	22.0356	22.0560	198	$2s^22p4p\ ^1P_1$		29.1039	28.9380	
28	$2s^22p3p\ ^3D_3$		22.2253	22.1128	22.1348	199	$2s^22p4p\ ^3D_2$		29.1062	28.9409	
29	$2s^22p3p\ ^3S_1$		22.2948	22.1739	22.1971	200	$2s^22p4p\ ^3P_0$		29.1524	28.9945	
30	$2s^22p3p\ ^3P_0$		22.3509	22.2032	22.2262	202	$2s^22p4p\ ^3D_3$		29.1828	29.0246	
31	$2s^22p3p\ ^3P_1$		22.3907	22.2521	22.2756	204	$2s^22p4p\ ^3S_1$		29.1886	29.0242	
32	$2s^22p3p\ ^3P_2$		22.4250	22.2820	22.3050	206	$2s^22p4p\ ^3P_1$		29.2371	29.0787	
33	$2s^22p3p\ ^1D_2$		22.7280	22.5690	22.5600	207	$2s^22p4p\ ^3P_2$		29.2490	29.0888	
34	$2s2p^23s\ ^5P_1$		22.9683			208	$2s^22p4p\ ^1D_2$		29.3129	29.1550	
35	$2s2p^23s\ ^5P_2$	22.9563	23.0073			211	$2s^22p4d\ ^3F_2$		29.4298	29.2586	
36	$2s2p^23s\ ^5P_3$	23.0130	23.0624			213	$2s^22p4p\ ^1S_0$		29.4357	29.2712	
37	$2s^22p3p\ ^1S_0$		23.0661	22.8915	22.8712	216	$2s^22p4d\ ^3F_3$		29.4670	29.2987	
38	$2s^22p3d\ ^3F_2$		23.1255	22.9832	22.9897	218	$2s^22p4d\ ^3D_2$		29.4849	29.3982	
39	$2s^22p3d\ ^3F_3$		23.1782	23.0382	23.0537	221	$2s^22p4d\ ^3D_1$		29.5203	29.3499	
40	$2s^22p3d\ ^1D_2$	23.0757	23.2087	23.0685	23.0775	223	$2s^22p4d\ ^3F_4$		29.5437	29.3744	
41	$2s^22p3d\ ^3F_4$		23.2379	23.1023	23.1286	226	$2s^22p4d\ ^1D_2$		29.5620	29.3118	
42	$2s^22p3d\ ^3D_1$	23.2229	23.3724	23.2202	23.2203	229	$2s^22p4d\ ^3D_3$	29.458	29.5925	29.4288	
43	$2s^22p3d\ ^3D_2$	23.2349	23.3858	23.2360	23.2428	231	$2s^22p4d\ ^3P_2$		29.6112	29.4478	
44	$2s^22p3d\ ^3D_3$	23.2868	23.4293	23.2811	23.2901	232	$2s^22p4d\ ^3P_1$		29.6166	29.4536	
45	$2s^22p3d\ ^3P_2$	23.3358	23.4680	23.3230	23.3326	233	$2s^22p4d\ ^3P_0$		29.6196	29.4571	
46	$2s^22p3d\ ^3P_1$	23.3476	23.4794	23.3366	23.3424	238	$2s^22p4d\ ^1P_1$		29.7068	29.5459	
47	$2s^22p3d\ ^3P_0$		23.4854	23.3448	23.3505	241	$2s^22p4d\ ^1F_3$	29.5565	29.7133	29.5492	

[a] Refers to the work of Landi & Bhatia (2003).

the $(N + 1)^{th}$ scattering electron for the four ions. All partial waves from J=0 to J=41 (S^{9+} and S^{11+}) or J=1/2 to J=81/2 (S^{8+} and S^{10+}) were included explicitly and the contribution from higher J-values were included using a "top-up" procedure (Burgess 1974, Badnell & Griffin 2001). The contributions from partial waves up to J=12 (S^{9+} and S^{11+}) or J=23/2 (S^{8+} and S^{10+}) were included in the exchange R-matrix, while those from J=13 to 41 or J=25/2 to 81/2 were included via a non-exchange R-matrix calculation. In the exchange calculation, a fine energy mesh ($1.0\times10^{-5}z^2$ Ryd, where z is the residual charge of ions) was used to resolve the majority of narrow resonances below the highest excitation threshold. From just above the highest threshold to a maximum energy of eight times the ionization potential for each ion, a coarse energy mesh ($1.0\times10^{-3}z^2$ Ryd) was employed. For the non-exchange calculation, a step of $1.0\times10^{-3}z^2$ Ryd was used over the entire energy range. Additionally, experimentally determined energies or adjusted energies were employed in the MQDT expressions used by the ICFT method to further improve the accuracy of the results, as was done for Si^{9+} (Liang et al., 2009a). The correction procedure was mainly done for levels of the n = 2 complex (needed because of the difficulty in obtaining a good structure here at the same time as describing n = 3 and 4 configurations with a unique orbital basis) and some levels of the $2s^22p^x3s$ (where x=3,2,1 or 0 for

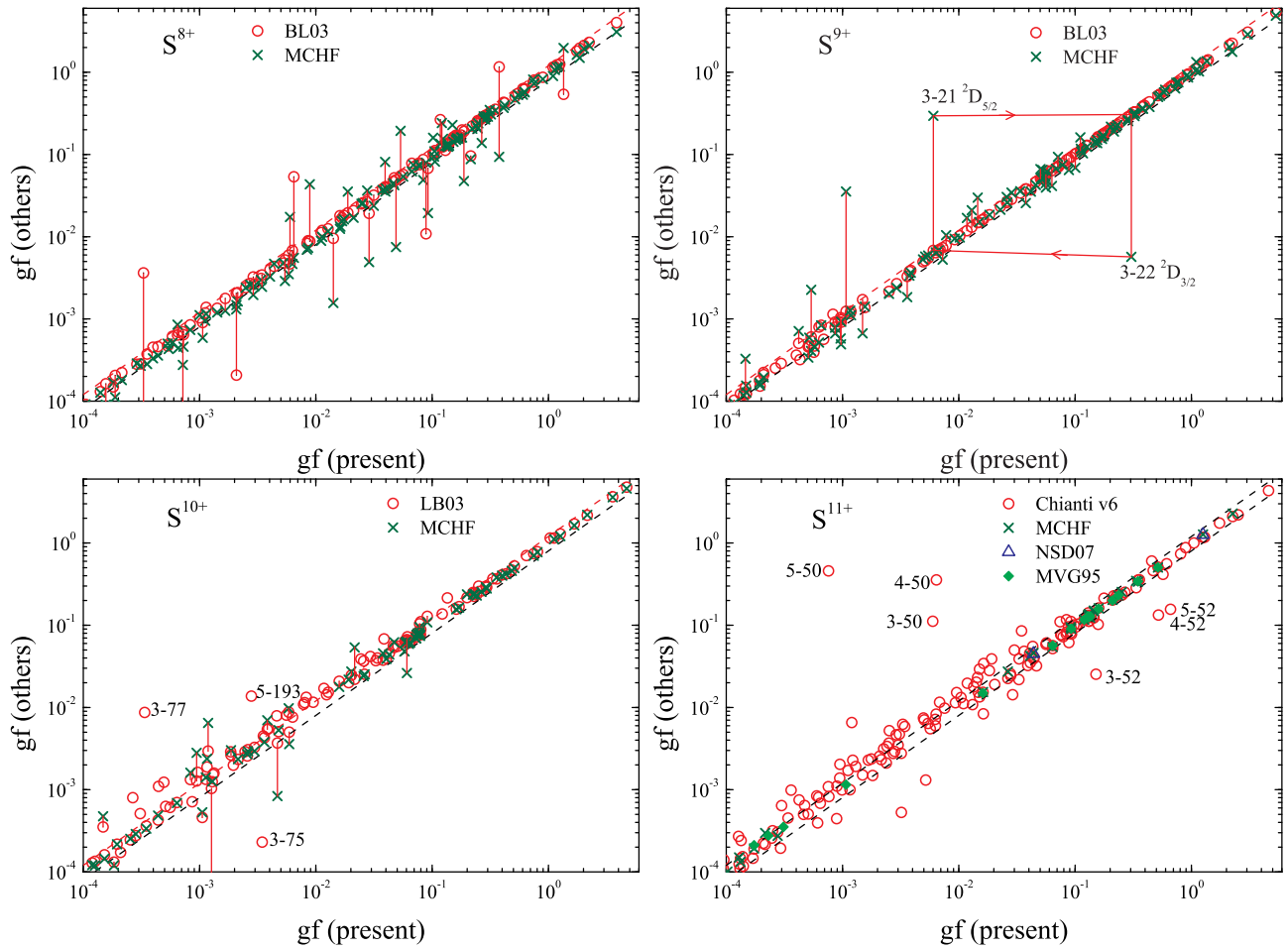

Fig. 1. Comparison of weighted oscillator strengths gf of electric-dipole transitions (to the 5 lowest-lying levels) for S^{8+} – S^{11+}. BL03 refers to the work of Bhatia & Landi (2003a; 2003b), whereas LB03 and NSD07 correspond to the work of Landi & Bhatia (2003) and Nataraj et al. (2007), respectively. The dashed lines correspond to agreement within 20%. [*Colour online*]

$S^{8+,9+,10+,11+}$, respectively) configuration, as explained in detail in the structure section.

We make use of the infinite energy Born limits (non-dipole allowed) or line strengths (dipole) to extend the *R*-matrix collision strengths to higher scattering energies by interpolation of reduced variables, as described by Burgess & Tully (1992). Finally, thermally averaged collision strengths (Υ) were generated at 13 electron temperatures ranging from $2\times10^2(z+1)^2$ K to $2\times10^6(z+1)^2$ K. The data were stored in the ADAS adf04 format (Summers, 2004) being available electronically from the OPEN-ADAS database [4], APAP-network [5] and the CDS archives [6].

5. Results and Discussions

5.1. S IX

In Fig. 2, we make an extensive comparison of the present effective collision strengths with the DW data of Bhatia & Landi (2003a) for excitations from the ground level $2s^22p^4\ ^3P_2$. At the low temperature ($\log T_e$ (K)=5.1), only 27% of transitions show agreement within 20%. This can be easily explained by the omission of resonances in the DW calculation by Bhatia & Landi (2003a). At the temperature ($\log T_e$ (K)=6.1) of peak fractional abundance in ionization equilibrium, the percentage is still low (41%). At the high temperature $\log T_e$ (K)=7.1), the percentage increases to 58%. This is due to the reduced contributions of near threshold resonances with increasing temperature. However, we note that there are a few transitions showing a ratio $\Upsilon_{BL03}/\Upsilon_{ICFT}$ >1.3, and the ratio increases with increasing temperature, e.g. the dipole transition of $2s^22p^4\ ^3P_2 \leftarrow 2s^22p^33d\ ^3P_1$ (1–80) marked by the dotted box in the lower-panel of Fig. 2. In the upper-panel of Fig. 2, we show the scaled collision strength as a function of reduced energy so as to shed light on this odd behaviour. The DW calculation by Bhatia & Landi (2003a) is higher than the background of the present ICFT *R*-matrix calculation and the present Breit–Pauli DW (hereafter AS-DW) calculation using AUTOSTRUCTURE (Badnell 2011). And the three different calculations show a self-consistent behaviour approaching the infinite-energy limit point. So the odd behaviour is due to the higher background in the DW calculation by Bhatia & Landi (2003a). The limit value from CHIANTI (v6) is also plotted, which shows an excellent agreement with present calculations. This inconsistency in the CHIANTI (v6) database is due to different data sources being adopted, e.g. the structure data is from a 24 configuration calculation, whereas the scattering data is from a 6 configuration calculation [7].

[5] http://www.apap-network.org
[6] http://cdsweb.u-strasbg.fr/cgi-bin/qcat?J/A+A/
[7] Landi, private communication (2011).

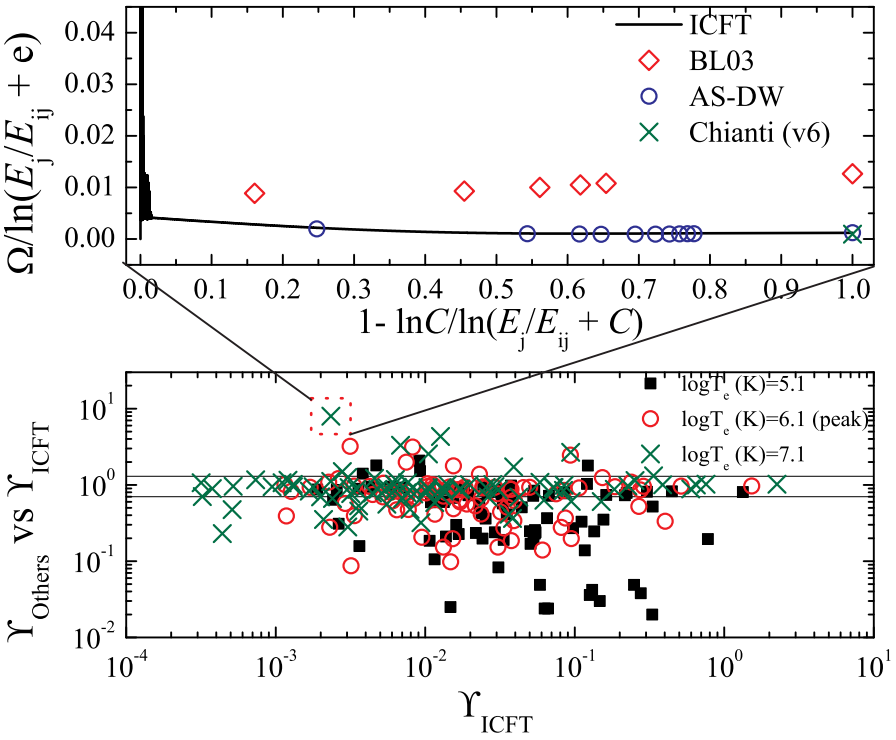

Fig. 2. Comparison of (effective) collision strengths (ϒs, see the *lower panel*) Ωs from the ground state of S^{8+}. BL03 refers to the distorted wave calculation by Bhatia & Landi (2003a), AS-DW refers to the present Breit–Pauli DW calculation using AUTOSTRUCTURE. *Upper panel:* scaled collision strength for a dipole transition $2s^22p^4\ ^3P_2 \leftarrow 2s^22p^33d\ ^3P_1$ (1–80) with C=2.0. The limit value is $4g_i f_{ij}/E_{ij}$ at 1.0 for the dipole transition. *Lower panel:* the ratio of ϒs between the results of theDW calculation by Bhatia & Landi (2003a) and the ICFT *R*-matrix calculation at logT_e (K) =5.1, 6.1 (corresponding to peak abundance of S^{8+} in ionization equilibrium) and 7.1. The dashed lines correspond to agreement within 20%. The transition marked by dotted box is the dipole transition 1–80 shown in the *upper panel*. [*Colour online*]

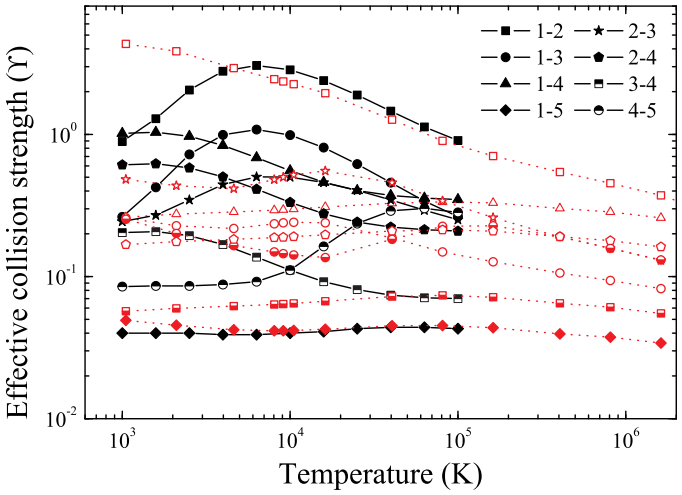

Fig. 3. Comparison of effective collision strengths of S^{8+} with the *R*-matrix results of Butler and Zeippen (1994) for transitions of the ground configuration $2s^22p^4$. Filled symbols with solid curves are results of Butler and Zeippen (1994), while open symbols with dotted curves corresponds to the present ICFT *R*-matrix calculation. *Note: The same symbol in the two sets of results corresponds to the same transition.* [*Colour online*]

For S^{8+}, an earlier *R*-matrix calculation for transitions within the ground configuration is available (Butler & Zeippen, 1994) for which the LS-coupling K-matrices were transformed algebraically to intermediate coupling to obtain collision strengths between the fine-structure levels. A detailed comparison has been made between the two different *R*-matrix calculations, see Fig. 3. At the low temperature ($T_e \sim 1.0 \times 10^4$K), there is a large difference between the two different *R*-matrix calculations. A separate ICFT *R*-matrix calculation with finer mesh ($1.0\times10^{-6}z^2$) near threshold confirms that the effect of resonance resolution is less than 2% for nearly all excitations, except for the 2–5 (10% at logT_e(K)=4.1) and 3–5 (24% at logT_e(K)=4.1) transitions. So the present effective collision strengths are generally converged with respect to resonance resolution. The large differences between the two different *R*-matrix calculations may be due to deficiencies in the transformational approach used by Butler & Zeippen (1994), as detailed by Griffin et al. (1998) and demonstrated by Liang et al. (2008). The adoption of observed energies for levels of n=2 complex in the present ICFT *R*-matrix calculation gives better positioning of near threshold resonances than the previous ones with theoretical energies (Butler & Zeippen, 1994). So, the present effective collision strengths are expected to be more reliable at low temperatures.

5.2. S X

In Fig. 4, an extensive comparison has been made with previous *R*-matrix calculation (Bell & Ramsbottom 2000) at three temperatures: logT_e(K)=5.2, 6.2 (corresponding to peak fraction in ionization equilibrium) and 6.7. At the low temperature (logT_e(K)=5.2), only 27% of all available transitions show an agreement within 20%. Even at the high tempera-

Table 7. Comparison of weighted oscillator strengths (gf) of S^{9+} between the previous data (Bhatia & Landi 2003a) and the present AUTOSTRUCTURE calculations with/without valence-valence two-body fine-structure interactions (TBFS) for the ground complex and level energy correction (labeled as LEC). The index number corresponds to that in Table 4. The last column is the data presented in Fig 1. *Note: only data with difference being > 20% are listed.*

			Present			
			With TBFS		Without TBFS	
i	j	BL03		LEC		LEC
1	10	4.176-6	4.240-6	1.330-5	6.685-6	9.749-6
1	13	1.195-4	1.222-4	1.410-4	1.392-4	1.225-4
1	19	1.214-4	1.207-4	1.483-4	1.232-4	1.455-4
1	20	1.526-4	1.518-4	1.951-4	1.415-4	2.084-4
1	32	2.007-6	1.979-6	1.035-6	1.315-6	1.722-6
1	56	1.386-8	1.478-8	9.315-7	3.075-7	2.317-7
1	76	8.706-5	8.684-5	6.689-5	8.707-5	6.677-5
1	77	7.970-4	7.942-4	6.280-4	7.364-4	6.882-4
1	83	1.856-7	1.603-7	1.601-5	2.091-6	7.996-6
1	84	3.191-7	3.229-7	5.315-7	3.216-0	1.255-8
2	7	1.198-5	1.196-5	1.608-5	1.347-5	1.464-5
2	20	8.382-4	8.311-4	6.546-4	8.107-4	7.251-4
2	59	2.976-5	2.927-5	3.587-5	2.142-5	4.579-5
4	7	2.021-6	2.014-6	2.426-6	2.116-6	2.311-6
4	16	4.998-5	4.956-5	6.865-5	4.955-5	6.868-5
4	17	1.237-4	1.222-4	1.487-4	1.222-4	1.486-4
5	8	1.704-6	1.686-6	9.851-7	1.309-6	1.323-6
5	9	1.227-4	1.256-4	1.323-4	1.264-4	1.625-4
5	17	5.655-4	5.599-4	6.878-4	5.443-4	7.040-4
5	18	2.940-6	2.848-6	2.795-6	4.540-6	1.326-6
5	51	2.586-5	2.574-5	1.494-5	2.086-5	2.190-5
5	58	1.141-3	1.133-3	8.269-4	1.026-3	9.380-4
5	59	3.933-4	3.888-4	5.672-4	4.425-4	5.000-4
5	61	3.205-4	3.171-4	4.305-4	3.524-4	3.855-4

Note: $x \pm y \equiv x \times 10^{\pm y}$.

ture ($\log T_e$(K)=6.7), the percentage is only about 34%. Ratios ($\frac{\Upsilon_{BR00}}{\Upsilon_{ICFT}}$) less than unity can be understood in terms of the finer energy mesh used (present: $1.0 \times 10^{-5} z^2$ Ryd, Bell & Ramsbottom 2000: ≥0.008 Ryd) and resonances attached to the $2s^2 2p^2 3l$ configurations in our present ICFT *R*-matrix calculation, as well as the purely algebraic JAJOM approach that was used by Bell & Ramsbottom (2000). However, the ratio being larger than unity requires another explanation. So, we select one transition marked by the bold '↘' in Fig. 4 to investigate the source of the difference between the two different *R*-matrix results.

Figure 5 shows a comparison of our present (effective) collision strength with the previous *R*-matrix results for the $2s^2 2p^3\ ^4S_{3/2} \leftarrow 2s2p^4\ ^2P_{3/2}$ (1–12) dipole transition. Around the temperature of $T_e \sim 9.0 \times 10^5$K – 6.0×10^6K, the Bell & Ramsbottom (2000) result is higher than present ICFT *R*-matrix calculation, and by up to a factor of 2. We note that some pseudo-orbitals ($\overline{3p}$, $\overline{4s}$, $\overline{4d}$ and $\overline{4f}$) were included in the work of Bell & Ramsbottom (2000). They stated that some pseudo-resonances are found above the highest threshold (19.682 Ryd). One of the authors (Ramsbottom, private communication, 2011) has provided us with collision strengths (Ω) with the pseudo-resonances at high energies removed. A comparison of the scaled collision strengths Ω reveals that the backgrounds of the two different *R*-matrix calculations agree well, and are consistent with the DW calculation by Bhatia & Landi (2003b). So, the large difference between the two different *R*-matrix calculations

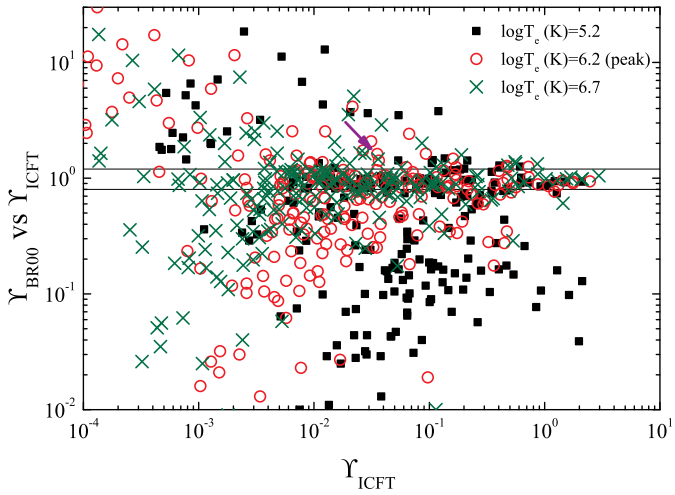

Fig. 4. Comparison of effective collision strengths of S^{9+} with the JAJOM *R*-matrix results of Bell & Ramsbottom (2000) for transitions of the $n = 2$ complex and $2s^2 2p^2 3s$ configuration. One point marked by bold '↘' refers to the $2s^2 2p^3\ ^4S_{3/2} \leftarrow 2s2p^4\ ^2P_{3/2}$ transition (1–12), that will be examined in Fig. 5. [*Colour online*]

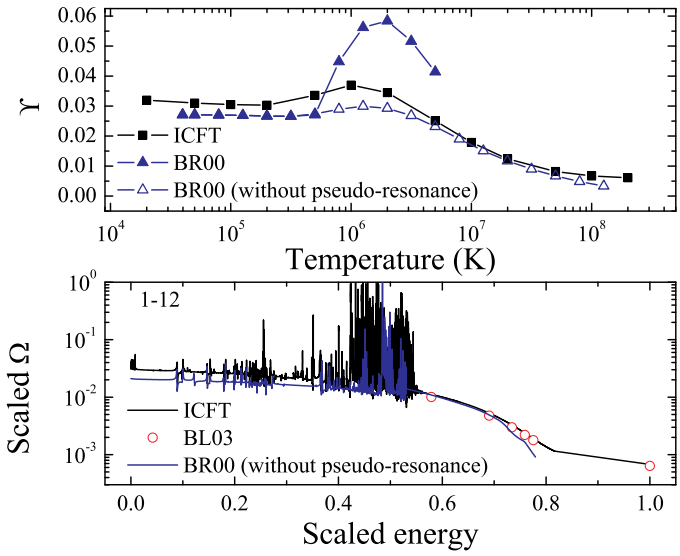

Fig. 5. Comparison of excitation data for the $2s^2 2p^3\ ^4S_{3/2} \leftarrow 2s2p^4\ ^2P_{3/2}$ transition (1–12) of S^{9+}. Here, BR00 refers to the *R*-matrix calculation of Bell & Ramsbottom (2000), BL03 to the DW result of Bhatia & Landi (2003b) and ICFT to the present calculation. *Upper panel:* Effective collision strengths — the BR00 without pseudo-resonances result was re-derived by us from the said original collision strengths provided by Ramsbottom (private communication, 2011). *Lower panel:* Scaled collision strengths, with the scaling parameter C set to 2.0. [*Colour online*]

is not arising from the difference in their structures. We then re-derived the effective collision strengths, which shows the expected behaviour, see Fig. 5. So, it appears that the previously published *R*-matrix effective collision strengths of Bell & Ramsbottom (2000) were derived from their collision strengths before the pseudo-resonances were subtracted. So, the ratios greater than unity in Fig. 4 should be mostly/partly attributed to

the pseudo-resonances in the previous *R*-matrix calculation. So, the present results are more reliable for modelling applications.

For excitations to higher levels of n=3 configurations, only DW data is available, e.g. the latest work of Bhatia & Landi (2003b). A comparison there demonstrates that the resonance contribution is strong for some transitions and is widespread, as expected. For conciseness, the figure is not shown here.

5.3. S XI

As mentioned in the introduction, interpolated data from *R*-matrix results is available for S^{10+} (Conlon et al. 1992). These resultant data are valid over a temperature range approximately equal to $T_e \sim 3.2 \times 10^5$ — 1.3×10^7K for S^{10+}. In this temperature range, the interpolated excitation data show a good agreement with present the ICFT *R*-matrix calculation for almost all transitions, as shown in Fig. 6, even though only partial waves of L <9 and 12 continuum basis orbitals in each channel were included. That is, the effective collision strength is converged in this temperature range using a small range of partial waves etc. Lennon & Burke (1994, hereafter LB94) performed an *R*-matrix calculation which included all 12 terms of the ground complex and adjusted the diagonal elements of the LS-coupling Hamiltonian matrix to the (fine-structure averaged) observed energies before diagonalization. They provided data for transitions between fine-structure levels in the ground configuration $2s^22p^2$ plus the $2s2p^3\ ^5S_2$. At low temperatures $T_e < 1.0 \times 10^5$K, the present ICFT *R*-matrix calculation is systematically higher than this previous small-scale *R*-matrix result except for the 1-6 transition, see Fig. 6. This situation can likely be attributed to the much larger close-coupling expansion (to n = 4) and associated resonances in the present calculation. We recall also that we used observed *level* energies in the present ICFT *R*-matrix calculation via multi-channel quantum defect theory (MQDT).

In case of the 1 – 6 transition, the original collision strength of Lennon & Burke (1994) is available from TIPTOPbase [8]. In figure 7, we compare the two sets of results. We see that there is a somewhat oddly high background around 0.5–2.0 Ryd in the results of Lennon & Burke (1994). This is the likely reason their effective collision strength is notably larger than the present one at lower temperatures.

Comparison with the DW calculation of Landi & Bhatia (2003) demonstrates that only 22% of all available transitions show agreement within 20%. Fig. 8 demonstrates that the resonance contribution is strong for some transitions, and widespread as expected again. At high temperature, uncertainties of scattering data are dominated by the accuracy of structure calculation because the resonance contribution becomes increasingly small. But only 43% of all available transitions show agreement within 20%, which is significantly lower than that in the assessment for weighted oscillator in section 3. We also notice there are a few transitions showing the ratio being larger than unity. So we select one transition ($2s^22p^2\ ^3P_0$ ← $2s^22p4p\ ^3P_0$, see the bold '↖' mark in Fig. 8-a) to investigate. Fig. 8 clearly demonstrates that the DW data of Landi & Bhatia (2003) is higher than the background of the present ICFT *R*-matrix calculation. But the present Breit–Pauli DW calculation using AUTOSTRUCTURE (Badnell 2011) shows an excellent agreement with the background of the *R*-matrix calculation — both use the exact same atomic structure. As stated by Landi & Bhatia (2003), a small atomic model (nine lowest configurations, 72 fine-structure levels) was adopted in their scattering calculation because of their available computer resource. So, we performed another separate AS-DW calculation with the 9 lowest configurations, in which the optimization procedure is done as mentioned above for S^{10+}. The resultant data show good agreement with the DW calculation by Landi & Bhatia (2003). So ratios lower than unity and the low percentage of agreement in the scatter plot mentioned above are likely due to the use of a much larger configuration interaction expansion in the present ICFT *R*-matrix calculation.

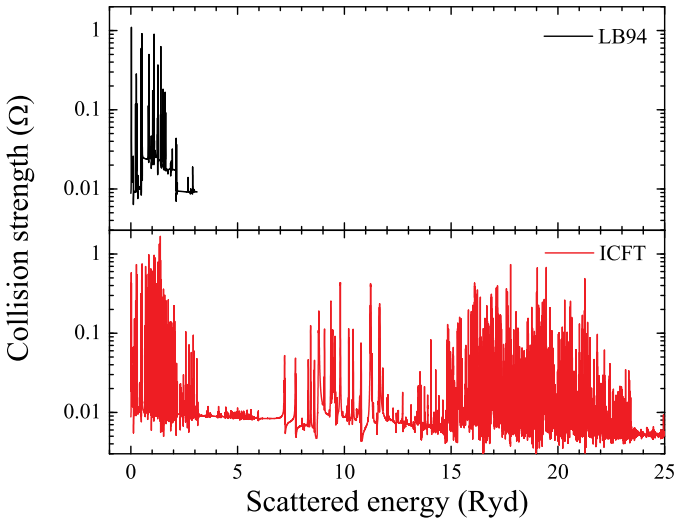

Fig. 7. Collision strengths (Ω) of the $2s^22p^2\ ^3P_0 \leftarrow 2s2p^3\ ^5S_2$ (1–6) transitions of S^{10+}, where LB94 corresponds to the *R*-matrix work of Lennon & Burke (1994) from the TIPTOPbase[8], ICFT denotes the present work. [*Colour online*]

5.4. S XII

As stated by Keenan et al. (2002), a small error in the previous excitation data (Zhang et al. 1994) was found for a few transitions of some boron-like ions, and those data were replaced. In Fig 9, we compare the present ICFT *R*-matrix excitation data with the revised data of Keenan et al. (2002) at three different temperatures ($\log T_e$(K)=6.04, 6.40 and 6.78) to check the validity of the present results or improvement by including larger CI and extensive close-coupling expansions. For strong excitations (≥0.1), a good agreement (within 20%) is obtained for most excitations (82%). For weak excitations, the present ICFT *R*-matrix results are systematically larger than previous ones except for a few transitions, e.g. 8–13 and 9–13. Indeed, the weaker the excitation, the greater the difference, and by more than a factor of 2 for a group of the weakest excitations. This can be easily explained by resonances attached to n=3 levels included in the present work, and this effect is stronger for weaker excitations. For the two above mentioned transitions (8–13 and 9–13), the previous *R*-matrix calculation is significantly higher than the present ones at $\log T_e$(K)=6.04 by a factor of 2.5 and 40%, respectively. Unfortunately, there are no previous collision strengths available to compare with — examination of the present collision strengths uncovers no untoward behaviour for these two transitions.

For excitations to higher excited levels of the n=3 configurations, only an unpublished DW calculation (Zhang & Sampson 1995) is available — compiled in the CHIANTI database. A com-

[8] http://cdsweb.u-strasbg.fr/topbase/home.html

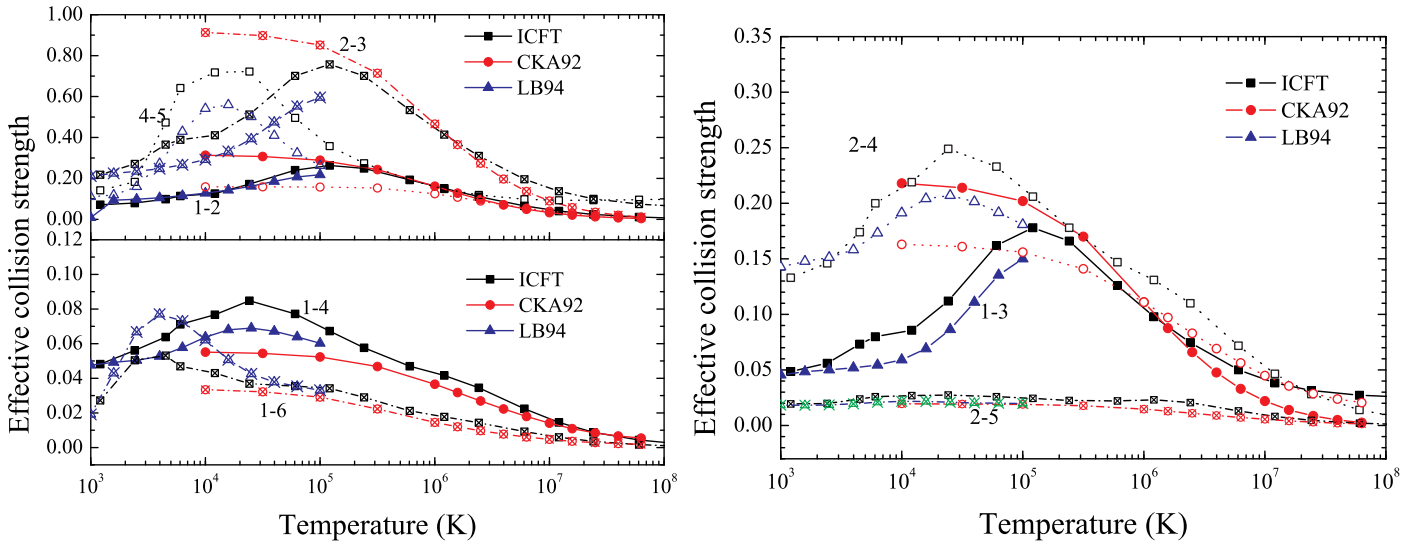

Fig. 6. Comparison of effective collision strengths between different *R*-matrix calculations for transitions in the ground configuration $2s^22p^2$ of S^{10+}, where CKA92 refers to the interpolated data from *R*-matrix results for other ions in carbon-like sequence (Conlon et al. 1992), LB94 corresponds to the *R*-matrix work of Lennon & Burke (1994), ICFT denotes the present work. The transition is marked by $i - j$ adjacent to the relevant set of curves. *Note: the CKA92 data is extracted from the* CHIANTI *v6 database.* [*Colour online*]

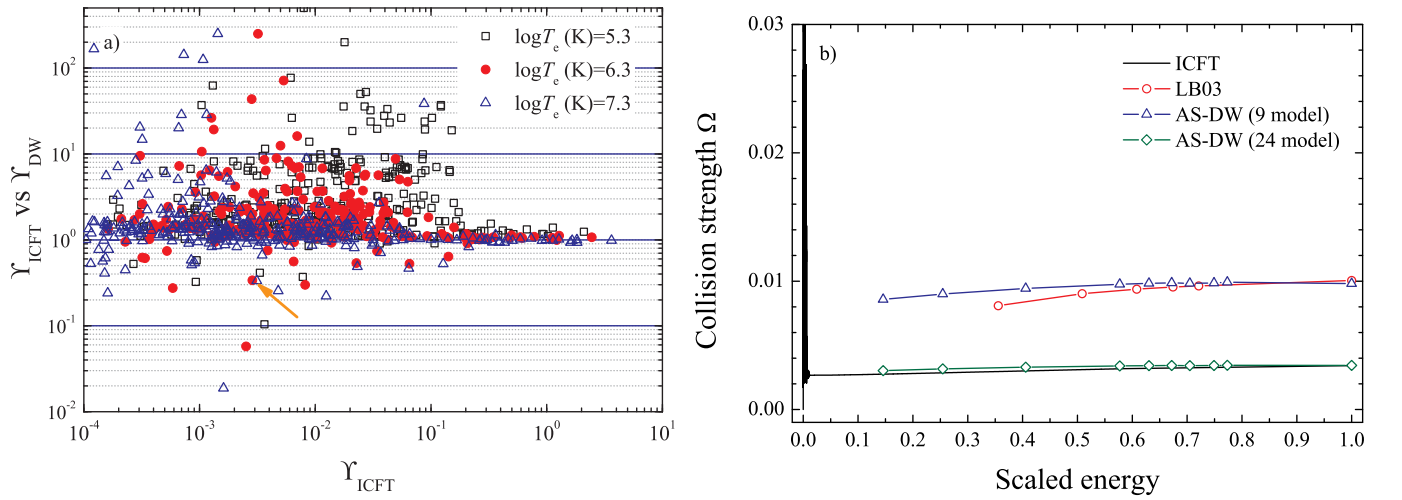

Fig. 8. Comparison of effective collision strengths of the present ICFT *R*-matrix results with other (DW) results. a) Scatter plot showing the ratio ($\frac{\Upsilon_{ICFT}}{\Upsilon_{DW}}$) for S^{10+} at three temperature of logT_e(K)=5.3, 6.3 and 7.3, where the DW calculation refers to the work of Landi & Bhatia (2003, LB03). The bold '↖' refers to a forbidden transition $2s^22p^2\ ^3P_0 \leftarrow 2s^22p4p\ ^3P_0$ transition (1–200), that is examined in panel b). b) Comparison of scaled collision strength Ω (with scaling parameter C=2.0) of the $2s^22p^2\ ^3P_0 \leftarrow 2s^22p4p\ ^3P_0$ transition (1–200). AS-DW (9 and 24 models) corresponds to the present Breit–Pauli DW calculation by using AUTOSTRUCTURE with 9 and 24 configurations, corresponding to that used in the scattering and structure calculations of Landi & Bhatia (2003), respectively. [*Colour online*]

parison demonstrates that the resonance contribution is strong for some transitions, and is widespread as expected. For conciseness, the figure is not shown here.

Additionally, we checked the sensitivity of the high-T_e ϒs to the top-up and find that it is greatest on the weakest (dipole) transitions but it is not significant compared to the inherent uncertainties in the atomic structure (f-values) for such transitions — the strong transitions are well converged.

6. Summary

Electron-impact excitation data for four iso-nuclear sulphur ions (S^{8+}, S^{9+}, S^{10+} and S^{11+}) have been calculated using the ICFT *R*-matrix method with extensive CI and large close-coupling expansions, as listed in Table 1.

Good agreement overall with the available experimentally derived data and other theoretical results for level energies and weighted oscillator strengths supports the reliability of the present *R*-matrix excitation data.

For excitations to levels of the n=2 complex, an extensive assessment have been made with previous *R*-matrix calculations

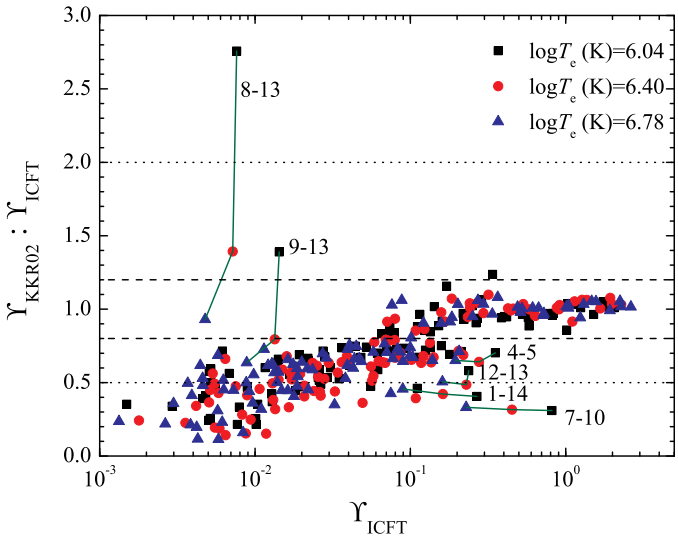

Fig. 9. Comparison of effective collision strengths of S^{11+} for all excitations between levels of the n=2 complex at three different temperatures logT_e(K)=6.04, 6.40 and 6.87. Υ_{ICFT} refers to the present ICFT *R*-matrix calculation, and KKR02 corresponds to the previous *R*-matrix results by Keenan et al. (2002). A few transitions with large difference are marked by labels around the points, and are linked together for results at different temperatures. [*Colour online*]

available to check the validity and improvement of the present ICFT *R*-matrix results. For excitations to higher excited levels of n=3 and/or 4 configurations, only DW calculations are available to compare with. The improvement of the present calculations is illustrated as expected by including resonances. For some transitions, configuration interaction has a significant effect on the atomic structure and this carries through to the final (effective) collision strengths, as shown in the cases of S^{8+} and S^{10+}.

In conclusion, the present ICFT *R*-matrix excitation data of $S^{8+,9+,10+}$ and S^{11+} are assessed to be valid over an extensive temperature range, and a significant improvement is achieved over previous available ones to date due to the extensive CI and large close-coupling expansions used in the present work. This will replace data from DW and small *R*-matrix calculations presently used by astrophysical and fusion communities, and its use can be expected to identify new lines, improve spectral analyses and diagnostics of hot emitters or absorbers in astrophysics and fusion researches.

Acknowledgements. The work of the UK APAP Network is funded by the UK STFC under grant no. PP/E001254/1 with the University of Strathclyde. GYL acknowledges the support from the One-Hundred-Talents programme of the Chinese Academy of Sciences (CAS), and thanks Dr Cathy Ramsbottom at Queen's University Belfast for providing her original electronic data as well as Dr Enrico Landi at University of Michigan for a helpful discussion. GZ and FLW acknowledges the support from National Natural Science Foundation of China under grant Nos. 10821061 and 10876040, respectively.

References

Acton, L.W., Bruner, M.E., Brown, W.A., et al. 1985, ApJ, 291, 865
Badnell, N.R. 1986, J. Phys. B: At. Mol. Opt. Phys., 19, 3827
Badnell, N.R. 2011, Comp. Phys. Comm., 182, 1528
Badnell, N.R., & Griffin, D.C. 2001, J. Phys. B: At. Mol. Opt. Phys., 34, 681
Bell, K.L., & Ramsbottom, C.A. 2000, At. Data and Nucl. Data Tables, 76, 176
Bhatia, A.K., & Landi, E. 2003a, At. Data and Nucl. Data Tables, 85, 169
Bhatia, A.K., & Landi, E. 2003b, ApJS, 147, 409
Brown, C.M., Feldman, U., Seely, J.F., Korendyke, C.M., & Hara, H. 2008, ApJS, 176, 511
Burgess, A. 1974, J. Phys. B: At. Mol. Opt. Phys., 7, L364
Burgess, A. & Tully, J.A. 1992, A&A, 254, 436
Butler, K., & Zeippen, C.J. 1994, Astron. Astrophys. Suppl. Ser., 108, 1
Conlon, E.S., Keenan, F.P., & Aggarwal, K.M. 1992, Physica Scripta, 45, 309
Dere, K.P., Landi, E., Young, P.R., Del Zanna, G., Landini, M., & Mason, E. 2009, A&A, 498, 915
Griffin, D.C., Badnell, N.R., & Pindzola, M.S. 1998, J. Phys. B: At. Mol. Opt. Phys., 31, 3713
Keenan, F.P., Katsiyannis, A.C., Ryans, R.S.I., et al. 2002, ApJ, 566, 521
Keenan, F.P., O'Shea, E., Thomas, R.J., et al. 2000, MNRAS, 315, 450
Landi, E., & Bhatia, A.K. 2003, ApJS, 149, 251
Lennon, D.J., & Burke, V.M. 1994, A&AS, 103, 273
Liang, G.Y., & Badnell, N.R. 2010, A&A, A518, A64
Liang, G.Y., & Badnell, N.R. 2011, A&A, A528, A69
Liang, G.Y., Whiteford, A.D., & Badnell, N.R. 2008, J. Phys. B: At. Mol. Opt. Phys., 41, 235203
Liang, G.Y., Whiteford, A.D., & Badnell, N.R. 2009a, A&A, 499, 943
Liang, G.Y., Whiteford, A.D., & Badnell, N.R. 2009b, A&A, 500, 1263
Merkelis, G., Vilkas, M.J., Gaigalas, G., & Kisielius, R. 1995, Physica Scripta, 51, 233
Nataraj, H.S., Sahoo, B.K., Das, B.P., et al. 2007, J. Phys. B: At. Mol. Opt. Phys., 40, 3153
Raassen, A.J.J., Mewe, R., Audard, M., et al. 2002, A&A, 389, 228
Summers, H.P. 2004 *The ADAS User manual version 2.6* http://www.adas.ac.uk/
Tachiev, G.I., & Froese Fischer, C. 2002, A&A, 385, 716
Thomas, R.J., & Neupert, W.M. 1994, ApJS, 91, 461
Witthoeft, M.C., Whiteford, A.D., & Badnell, N.R. 2007, J. Phys. B: At. Mol. Opt. Phys., 40, 2969
Zhang, H.L., Graziani, M., & Pradhan, A.K. 1994, A&A, 283, 319

Table 6. Level energies (Ryd) of S^{11+} from different calculations along with experimentally derived values from NIST v4. *Note: only levels with available NIST data and other predictions are listed. The complete table can be available from CDS archives.*

ID	Specification	NIST[1]	AS	CHIANTI[a]	NSD07[b]	ID	Specification	NIST	AS	CHIANTI[a]	NSD07[b]
1	$2s^22p\ ^2P_{1/2}$		0.0000			54	$2s2p3d\ ^2F_{5/2}$	27.322	27.4185	27.2824	
2	$2s^22p\ ^2P_{3/2}$	0.119698	0.1185	0.1197[x]	0.1227	55	$2s2p3d\ ^2F_{7/2}$	27.396	27.4896	27.3578	
3	$2s2p^2\ ^4P_{1/2}$	1.76678	1.7295	1.7668[x]	1.7656[y]	56	$2s2p3d\ ^2P_{3/2}$	27.443	27.5264	27.3679	
4	$2s2p^2\ ^4P_{3/2}$	1.81046	1.7733	1.8105[x]	1.8093[y]	57	$2s2p3d\ ^2P_{1/2}$	27.477	27.5669	27.4098	
5	$2s2p^2\ ^4P_{5/2}$	1.87197	1.8394	1.8720[x]	1.8702[y]	58	$2s2p3p\ ^2P_{1/2}$		27.8631	27.7804	
6	$2s2p^2\ ^2D_{3/2}$	3.1594	3.1941	3.1594[x]	3.1461[y]	59	$2s2p3p\ ^2P_{3/2}$		27.8800	27.7947	
7	$2s2p^2\ ^2D_{5/2}$	3.16214	3.1988	3.1621[x]	3.1493[y]	60	$2s2p3p\ ^2D_{3/2}$	27.894	27.9040	27.8174	
8	$2s2p^2\ ^2S_{1/2}$	4.0057	4.0522	4.0057[x]	3.9887[y]	61	$2s2p3p\ ^2D_{5/2}$	27.894	27.9057	27.8174	
9	$2s2p^2\ ^2P_{1/2}$	4.23516	4.3012	4.2352[x]	4.2260[y]	62	$2s2p3p\ ^2S_{1/2}$		28.1199	28.0381	
10	$2s2p^2\ ^2P_{3/2}$	4.2960	4.3666	4.2960[x]	4.2864[y]	63	$2p23s\ ^4P_{1/2}$		28.3086	28.2094	
11	$2p^3\ ^4S_{3/2}$	5.55941	5.5632	5.5594[x]	5.5529[y]	64	$2p23s\ ^4P_{3/2}$		28.3510	28.2527	
12	$2p^3\ ^2D_{3/2}$	6.2869	6.3534	6.2869[x]	6.2603[y]	65	$2p23s\ ^4P_{5/2}$		28.4161	28.3157	
13	$2p^3\ ^2D_{5/2}$	6.2921	6.3634	6.2921[x]	6.2645[y]	66	$2s2p3d\ ^2F_{7/2}$		28.6562	28.5654	
14	$2p^3\ ^2P_{1/2}$	7.0534	7.1496	7.0534[x]	7.0243[y]	67	$2s2p3d\ ^2F_{5/2}$	28.506	28.6584	28.5682	
15	$2p^3\ ^2P_{3/2}$	7.06966	7.1678	7.0697[x]	7.0398[y]	68	$2s2p3d\ ^2D_{3/2}$		28.7631	28.6427	
16	$2s23s\ ^2S_{1/2}$		23.2974	23.1956	23.3186	69	$2s2p3d\ ^2D_{5/2}$	28.620	28.7763	28.6548	
17	$2s23p\ ^2P_{1/2}$		24.1824	24.0825	24.2053	70	$2p23s\ ^2P_{1/2}$		28.8013	28.6888	
18	$2s23p\ ^2P_{3/2}$		24.2153	24.1162	24.2386	71	$2p23s\ ^2P_{3/2}$		28.8704	28.7571	
19	$2s23d\ ^2D_{3/2}$	25.036	25.0526	24.9441	25.0837	72	$2s2p3d\ ^2P_{1/2}$		28.9214	28.8042	
20	$2s23d\ ^2D_{5/2}$	25.043	25.0624	24.9536	25.0926	73	$2s2p3d\ ^2P_{3/2}$		28.9346	28.8142	
21	$2s2p3s\ ^4P_{1/2}$		25.1340	25.0355		74	$2p23p\ ^2S_{1/2}$		28.9545	28.8417	
22	$2s2p3s\ ^4P_{3/2}$		25.1728	25.0740		75	$2p23p\ ^4D_{1/2}$		29.0458	28.9315	
23	$2s2p3s\ ^4P_{5/2}$	25.285	25.2443	25.1480		76	$2p23p\ ^4D_{3/2}$		29.0716	28.9572	
24	$2s2p3s\ ^2P_{1/2}$		25.5847	25.4734		77	$2p23s\ ^2D_{5/2}$		29.0868	29.0118	
25	$2s2p3s\ ^2P_{3/2}$		25.6643	25.5546		78	$2p23s\ ^2D_{3/2}$		29.0915	29.0156	
26	$2s2p3p\ ^4D_{1/2}$		25.9258	25.8279		79	$2p23p\ ^4D_{5/2}$		29.1157	29.0016	
27	$2s2p3p\ ^4D_{3/2}$		25.9617	25.8625		80	$2p23p\ ^4D_{7/2}$		29.1757	29.0608	
28	$2s2p3p\ ^2P_{1/2}$	25.886	25.9950	25.9018		81	$2p23p\ ^4P_{1/2}$		29.1961	29.0807	
29	$2s2p3p\ ^2P_{3/2}$	25.953	26.0102	25.9171		82	$2p23p\ ^4P_{3/2}$		29.2084	29.0907	
30	$2s2p3p\ ^4D_{5/2}$		26.0225	25.9227		83	$2p23p\ ^4P_{5/2}$		29.2434	29.1265	
31	$2s2p3p\ ^4D_{7/2}$		26.0858	25.9892		84	$2p23p\ ^2D_{3/2}$		29.3169	29.1974	
32	$2s2p3p\ ^4S_{3/2}$		26.1845	26.0807		85	$2p23p\ ^2D_{5/2}$		29.3979	29.2818	
33	$2s2p3p\ ^4P_{1/2}$		26.2653	26.1647		86	$2p23p\ ^2P_{3/2}$		29.5566	29.4369	
34	$2s2p3p\ ^4P_{3/2}$		26.3044	26.2043		87	$2p23p\ ^2P_{1/2}$		29.5699	29.4480	
35	$2s2p3p\ ^4P_{5/2}$		26.3375	26.2349		88	$2p23p\ ^4S_{3/2}$		29.6045	29.3999	
36	$2s2p3p\ ^2D_{3/2}$	26.388	26.4104	26.3067		89	$2p23d\ ^4F_{3/2}$		29.7270	29.6128	
37	$2s2p3p\ ^2D_{5/2}$	26.468	26.4831	26.3827		100	$2p23d\ ^2F_{5/2}$		30.0001	29.8983	
38	$2s2p3d\ ^4F_{3/2}$		26.6901	26.5796		101	$2p23d\ ^2P_{1/2}$		30.0173	29.8852	
39	$2s2p3d\ ^4F_{5/2}$		26.7135	26.6030		102	$2p23d\ ^2F_{7/2}$		30.0834	29.9856	
40	$2s2p3p\ ^2S_{1/2}$	26.698	26.7294	26.6255		103	$2p23p\ ^2D_{3/2}$		30.1533	29.9758	
41	$2s2p3d\ ^4F_{7/2}$		26.7479	26.6388		104	$2p23p\ ^2D_{5/2}$		30.1562	29.9741	
42	$2s2p3d\ ^4F_{9/2}$		26.7970	26.6920		105	$2p23d\ ^4P_{5/2}$		30.1599	30.0059	
43	$2s2p3d\ ^4D_{1/2}$		26.9396	26.8016		122	$2p23p\ ^2P_{1/2}$		31.1471	31.0749	
44	$2s2p3d\ ^4D_{3/2}$	26.903	26.9407	26.8021		123	$2p23p\ ^2P_{3/2}$		31.1607	31.0883	
45	$2s2p3d\ ^4D_{5/2}$	26.890	26.9417	26.8024		129	$2s24d\ ^2D_{3/2}$	32.289	32.3629		
46	$2s2p3d\ ^2D_{3/2}$		26.9844	26.8391		130	$2s24d\ ^2D_{5/2}$	32.289	32.3668		
47	$2s2p3d\ ^4D_{7/2}$	26.952	26.9908	26.8553		149	$2s2p4p\ ^2D_{5/2}$	34.008	34.1315		
48	$2s2p3s\ ^2P_{1/2}$		26.9965	26.9334		159	$2s2p4d\ ^4D_{7/2}$	34.209	34.2968		
49	$2s2p3d\ ^2D_{5/2}$	26.943	26.9981	26.8553		172	$2s2p4d\ ^2F_{5/2}$	34.325	34.4282		
50	$2s2p3s\ ^2P_{3/2}$		27.0021	26.9344		177	$2s2p4d\ ^2F_{7/2}$	34.370	34.4854		
51	$2s2p3d\ ^4P_{5/2}$	27.008	27.0528	26.9209		193	$2s2p4d\ ^2F_{7/2}$	35.84	35.9979		
52	$2s2p3d\ ^4P_{3/2}$	27.036	27.0622	26.9367		194	$2s2p4d\ ^2F_{5/2}$	35.84	35.9981		
53	$2s2p3d\ ^4P_{1/2}$		27.0702	26.9457		204	$2s2p4f\ ^2D_{5/2}$		36.2258		

[a] Refers to the theoretical value in CHIANTI v6.
[b] NSD07 corresponds to the prediction of Nataraj et al. (2007) with relativistic coupled-cluster theory.
[x] These data are found to be observed, after checking the original paper (Zhang et al. 1994).
[y] Data are from the work of Merkelis e al. (1995) by using many-body perturbation theory (MBPT).